Molecular modelling reveals mode of interaction of γ-tubulin with the microtubules

Charu Suri[1], Rajesh K. Meher[1], Harish C. Joshi[2] and Pradeep Kumar Naik[3*]

[1]Department of Biotechnology and Bioinformatics, Jaypee University of Information Technology, Waknaghat, Distt. Solan 173234, Himachal Pradesh, India.

[2]Department of Cell Biology, 447 Whitehead Biomedical Research Building, Emory University School of Medicine, Atlanta, GA, 30322, United States

[3]Department of Biotechnology & Bioinformatics, Sambalpur University, Jyoti Vihar – 768 019, Sambalpur, Odisha, India

* Corresponding authors

E-mail: pknaik1973@gmail.com, Phone: +91-9479268802

Abstract

γ-tubulin is a small globular protein, found to be localised at the microtubule organizing centers. It is experimentally observed to interact with the minus end of microtubules to facilitate the nucleation and organization of mitotic microtubules in dividing cells. The most well accepted hypothesis for the initiation of microtubule polymerization is that α/β-tubulin dimers add onto a γ-tubulin ring complex (γTuRC), in which adjacent γ-tubulin subunits bind to the underlying non-tubulin components of the γTuRC. This template determines the resulting microtubule lattice. In this study we use molecular modelling and molecular dynamics simulations, combined with computational MM-PBSA/MM-GBSA methods, to determine the extent of the atomic interaction of γ-tubulin (though one of its horizontal interface) with microtubules. We first prepared the molecular system comprising of γ-tubulin, microtubule represented by α/β tubulin and GCP4 using protein-protein docking algorithm. We then MD simulated the complex to check its stability through 10 ns of simulation. We calculated the ensemble average of binding free energy of -110.86 kcal/mol by the MM-PBSA method and 120.42 kcal/mol by the MM-GBSA method. These highly favourable binding free energy values imply robust interaction of γ-tubulin with microtubules. Next we identified the hot spot amino acids that play key role in the interactions by computational alanine scanning mutagenesis and free energy decomposition per residue. Experimental mutagenesis validated these hot spot amino acids. The results from the experimental findings were consistent with the theoretical calculations and offer important insights on the mechanism of interaction between the γ-tubulin and microtubules.

Keywords: Gamma tubulin, microtubules, molecular modelling, Md simulation, MM-PBSA, MM-GBSA, alanine scanning mutation

Introduction

'Template model' of nucleation suggests that the γ-tubulins in the γTuRC function as a microtubule template, making lateral contacts with each other around the ring and longitudinal contacts with α-tubulin (minus end of the microtubule). The γTuRC was shown to interact specifically with microtubule minus ends, at which it functions as a cap to prevent microtubule growth in the minus direction [1]. This was consistent with electron micrograph images showing closed structures at the ends of microtubules, whether nucleated by γTuRCs *in vitro* [1-3] or attached to MTOCs *in vivo* [4]. According to this model γ-tubulin directly interacts, via one of its longitudinal interfaces, with the GCP2, GCP3 or GCP4 and, via its other interface, with the α/β tubulin dimers.

A major advance toward the full understanding of γ-tubulin complexes was achieved by the determination of the crystal structure of monomeric human γ-tubulin bound to GTP and to GDP [5, 6] and more recently that of human GCP4 [7]. Also, recent 8 A^0 resolution electron density map of a tetramer sub-complex containing two hetero-dimers of γ-tubulin and GCP4 [7] is a very welcome and timely beginning in the precise understanding of the binding interfaces of γ-tubulin, on its interface with components of the γTuRC.

In this study we use the knowledge of known structures to first obtain a complex of γ-tubulin with α/β tubulin and GCP4 using protein-protein docking. We then MD simulated the resultant molecular system for 10 ns. Further binding free energy was calculated to elucidate the strength of interaction of γ-tubulin with α/β tubulin

Materials and Methods

Molecular system

A pseudo atomic model of the α/β tubulin tetramer was obtained from David B. Wells from University of Illinois, Urbana, Illinois while the coordinated of GCP4 and γ-tubulin tetramer was obtained from Georges Czaplicki, from the Universite´ de Toulouse, UPS, Toulouse, France (Figure 1). As γ-tubulin interacts with α/β tubulin at the minus end, we deleted one of the β-tubulin to obtain the seam conformation. Since no crystal structure of the complete complex (comprising of α/β tubulin, γ-tubulin and GCPs) is known, we followed a two step process that involved initial protein-protein docking using Zdock (version 2.3) followed by refinement of docked complex using Rdock.

Zdock is a rigid-body docking algorithm based on the principle of pair wise shape complementarity (PSC), electrostatic and desolvation parameters [9]. In step 2, the top scoring poses obtained from Zdock were energy minimized using CHARMM force field. The binding affinity ($\Delta G_{binding}$) between the protein complexes was predicted using Rdock scoring function which is the sum of desolvation and electrostatics contribution.

$$\Delta G_{binding} = \Delta G_{ACE} + \beta \text{ X } \Delta G_{elec}$$

where β is a scaling factor, a value of 0.9 was used in this study. The conformation with least RDock score was then selected for further molecular dynamics studies [10].

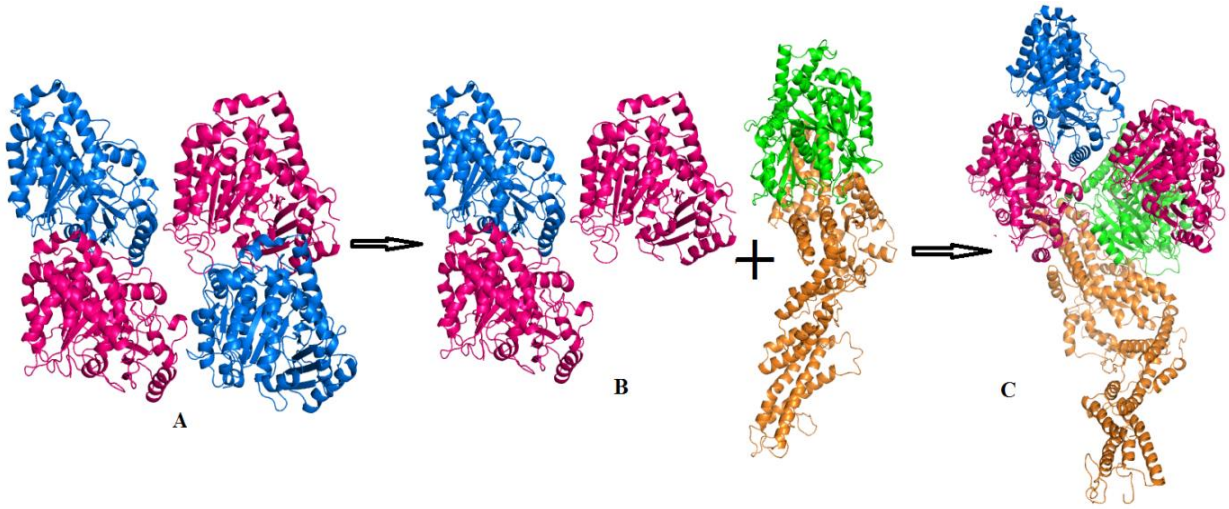

Figure 1: Preparation of molecular system. A: The coordinates of 'α/β tubulin tetramer obtained from David B. Wells *et.al*. from University of Illinois. B: Protein complexes for docking. C: The resulting docked complex obtained after Rdock. In the figure α-tubulin is shown as magenta cartoon, β-tubulin as blue cartoon, γ-tubulin as green cartoon and GCP4 as orange cartoon.

Molecular Dynamics Simulation

To further refine the structure, a small run of all atom Molecular Dynamics (MD) simulations was carried out for 1000 ps with a time step of 2 fs on the modelled structure using Gromacs package (Version 4.5.4) [11]. The simulations were set up with Amber99SB force field [12], in a dodecahedron solvation box at a distance of 12Å from the periphery of the protein with TIP3P water molecules, using periodic boundary conditions [13]. Particle-Mesh-Ewald algorithm was employed to calculate the electrostatic interactions between atoms [14, 15]. The Lenard-Jones and electrostatic interaction cut-off were set at 1.0 nm distance. LINCS algorithm was used to

constraint the bond lengths [16]. Prior to the 10 ns MD Simulation the molecular system was neutralized with 36 Na+ ions, energy relaxed using steepest descent algorithm for 1000 steps and then equilibrated for 1000 ps of MD run. An average structure was generated using the last 2000 frames from the total of 10,000 frames generated during MD simulation.

Calculation of binding free energy between γ-tubulin and microtubules

The average structure obtained after simulation in gromacs was first minimised, equilibrated for 500 ps followed by 5ns MD simulation using Amber 11.0 and Ambertools 1.5 [17, 18] for γ-tubulin dimer. Binding free energy calculations were carried out using the conventional MM-PBSA and MM-GBSA approaches using Amber 11 [19, 20]. A total of 200 snapshots were extracted, every 10 ps from the 5 ns of the MD trajectory. For each snapshot, the free energy was calculated for each molecular species (complex, protein and ligand). Conceptually the binding free energy can be calculated as :

$$\Delta G_{bind} = \Delta G_{complex} - [\Delta G_{Rec} + \Delta G_{lig}]$$
$$G = E_{gas} + G_{sol} - TS.$$
$$E_{gas} = E_{int} + E_{ele} + E_{vdw}$$
$$G_{sol} = G_{PB(GB)} + G_{sol-np}$$
$$G_{sol-np} = \gamma SAS$$

Where, **G** is Gibbs free energy, E_{gas} is the gas phase energy calculated as the sum of internal energy (E_{int}), energy generated as a result of the electrostatic interaction (E_{ele}) and the van der Waals interaction (E_{vdw}). G_{sol} is the solvation free energy calculated as the sum of polar ($G_{PB(GB)}$) and nonpolar contributions (G_{sol-np}). Polar interaction contribution ($G_{PB(GB)}$) was calculated as the summation of electrostatic contribution (E_{ele}) and polar solvation contribution ($G_{PB(GB)}$). The nonpolar solvation contribution (G_{sol-np}) is approximated as linearly dependent on the solvent accessible surface area (SAS) and γ is the surface tension constant that was set to 0.0072 kcal mol^{-1} $Å^{-2}$ [21].

Per residue energy contribution

Energy decompostion method, implemented in Amber 11, was employed on the 200 frames extracted every 10 ps from 2 ns of simulation using the MM-GBSA method. The residues contributing more than -2 kcal/mol were considered very significant for the binding of GCP4 with γ-tubulin and these residues were designated as hotspot amino acids.

Computational Alanine Scanning Mutagenesis

To further study the energy contribution of these amino acids in the interaction of α/β tubulin and γ-tubulin, computational alanine scanning was performed. In this method an amino acid of interest is replaced with alanine and absolute binding free energy is recalculated. For our study we also identified those amino acids which contributed significantly to the binding of α/β tubulin and γ-tubulin and were flanked by two or more polar amino acids. Four such segments were identified as shown in figure 2. Corresponding to each segment, four mutant structures were prepared by mutating the polar amino acids in these stretches into alanine. Each of the four mutants were then MD simulated in Amber for 5ns.

Experimental alanine scanning mutation and phenotypes

pALTER-EX1 vector (Promega, Madison, WI) was used to subclone *TUBG1* cDNA into the *NdeI* site downstream from the SP6 promoter to create pTWH101 as described by Hendrickson *et al*.[22]. Based on our findings from the molecular modelling methods, 4 stretches of polar amino acids were identified as shown in figure 2. The amino acids in each of the four stretches were mutated to alanine by oligonucleotide-directed mutagenesis using pTWH101 as the template. pALTER-EX1 contains a tetracycline resistance gene and an inactivated ampicillin resistance gene to obtain four mutants. The ampicillin-repair oligonucleotide restores the activity of the inactivated AmpR gene, and the tetracycline knockout oligonucleotide inactivates the TetR gene. This schema, i.e., inactivation of the TetR gene and the activation of the AmpR gene, provided a rapid method for selecting potential alanine-scanning mutants. Because contiguous alanine codons can be used to create a *PstI* site, we used *PstI* digestion to further screen for potential alanine-scanning mutants. We then verified the mutated sequences that represented the only differences between the mutant (*tubg1*) and the wild type (*TUBG1*).

The yeast expression plasmids were constructed by subcloning each of the *tubg1* alleles into pREP1 at the *NdeI* site downstream of the *nmt1+* promoter[23, 24]. Wildtype cells[25] were transformed with either one of the *tubg1*-pREP1 plasmids or the control *TUBG1*-pREP1 and grown in minimal media supplemented with adenine, histidine, and uracil. Transformants were screened at 18 and 36 °C to identify conditional mutants in the presence of endogenous γ-tubulin. The strains were maintained at 30 and 26 °C, respectively. A diploid strain, NC377[26, 27], bearing one endogenous wild-type copy of *S. pombe* γ-tubulin, *gtb1+* and one disrupted copy, *gtb1::ura4+*, was also

transformed with the mutant plasmids. The resulting yeast transformants were randomly sporulated and selected for *ura+*, *leu+*, and the spores were tested for conditional growth.

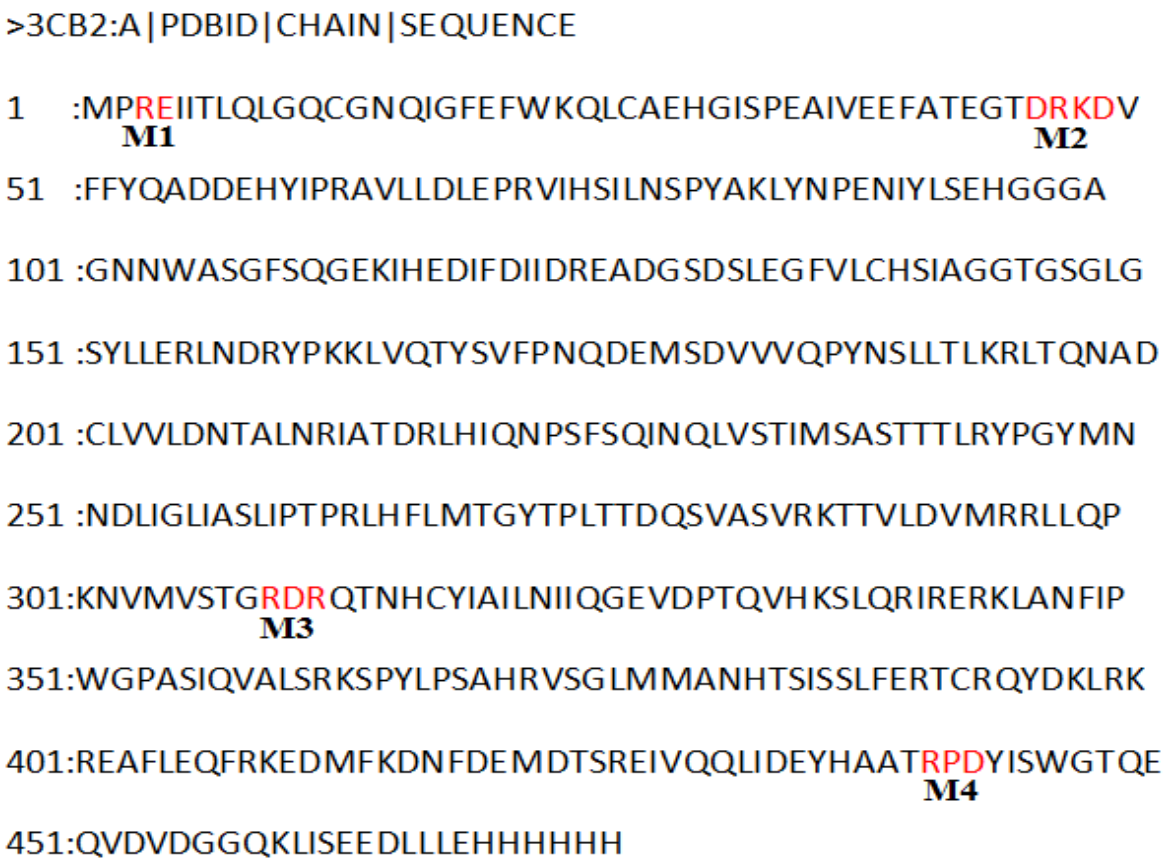

Figure 2: Amino acid stretches identified for alanine scanning mutagenesis. A total of seven stretched were identified on the basis of individual amino acid contribution and their participation interaction with α/β tubulin.

Results and discussions

Preparation of Molecular system

A total of 2,000 conformations, categorized into 100 clusters, were generated after Zdock. On the basis of Zdock score and visual inspection to rule out unfavourable conformations, 132 conformations were selected for Rdock. A total of 79 conformations were found to have favourable Rdock score of which the conformation with least energy was obtained for molecular dynamics (Figure 3). After Rdock, the selected conformation was then simulated for 10 ns in Gromacs. Root mean square deviation (RMSD) analysis reveals a very stable structure throughout 10 ns of simulation (Figure 4). An average structure was obtained from last 2 ns of simulation. The average

structure was then minimised and checked for structure quality. The overall quality of the model obtained, stereo-chemical values and non-bonded interactions were tested using PROCHECK, ERRAT and VERIFY3D [28-31].

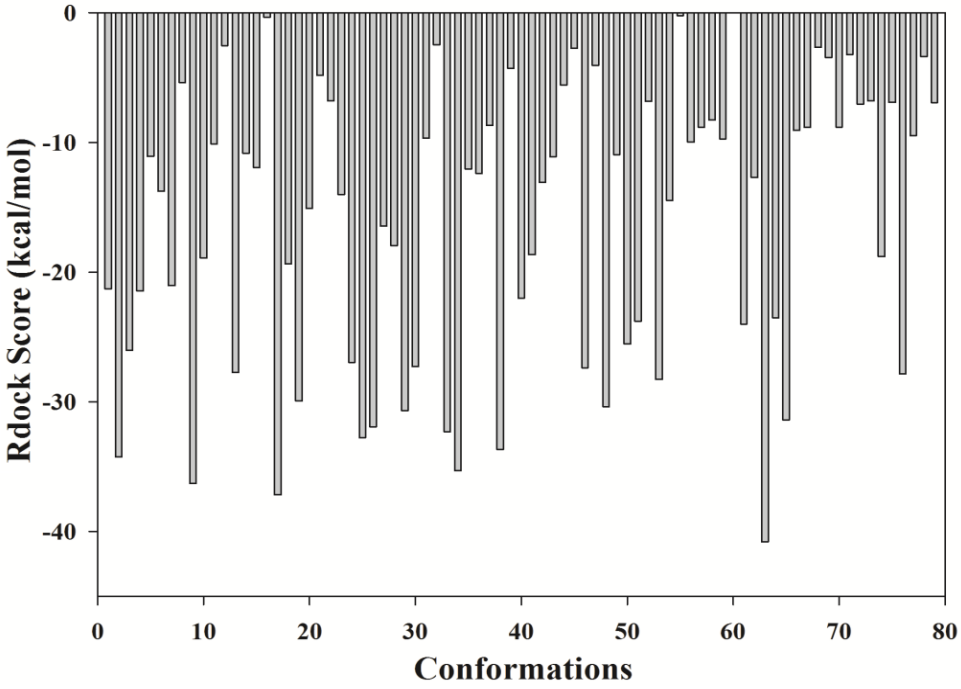

Figure 3: Comparison of $\Delta G_{binding}$ energy of different docking complexes between α/β tubulin and γ-tubulin calculated using Rdock.

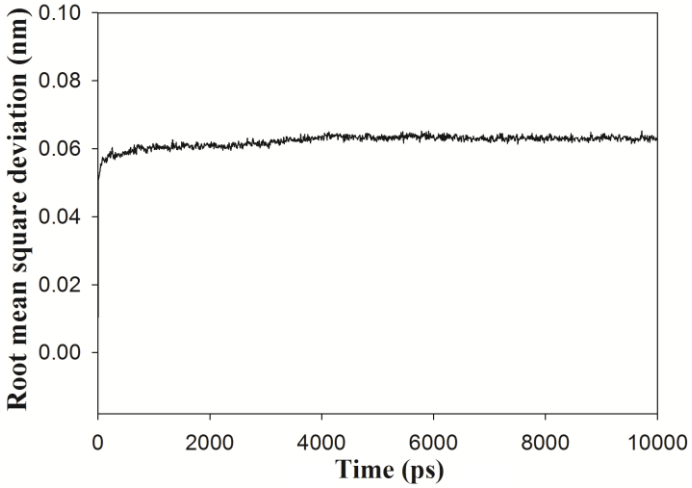

Figure 4: Root mean square deviation (RMSD) estimated over 10 ns. The RMSD was very stable around 0.06 nm throughout the simulation.

The PROCHECK results showed 99.5 % of backbone angles are in allowed regions with G-factors of - 0.25. Ramachandran plot analysis revealed only 0.5% residues in the generously allowed region and no residue in the disallowed region. ERRAT is an "overall quality factor" calculator program for non-bonded atomic interactions. The accepted range in ERRAT is 50 and higher scores indicate the precision of the model. For a structure with a resolution between 2.5Å– 3Å, the average structure quality is 91%. For the minimized average structure the ERRAT score was 91.43% that is within the range of high quality model. Similarly, VERIFY3D Determines the compatibility of an atomic model (3D) with its own amino acid sequence (1D) by assigned a structural class based on its location and environment (alpha, beta, loop, polar, nonpolar etc) and comparing the results to good structures. The structure passed the VERIFY3D test which implies at least 80% of the amino acids scored >= 0.2 in the 3D/1D profile.

Molecular Dynamics Simulation

The minimized molecular system was again simulated using Amber11 for 5ns. Mutant structures were prepared by mutating the identified polar amino acids (as indicated in figure 2) into alanine. All four mutants were also MD simulated in amber for 5 ns. Root mean square deviation analysis indicated that all complexes except Mutant 3 stabilized after 2 ns (Figure 5). Mutant 3 also showed stability after 3ns.

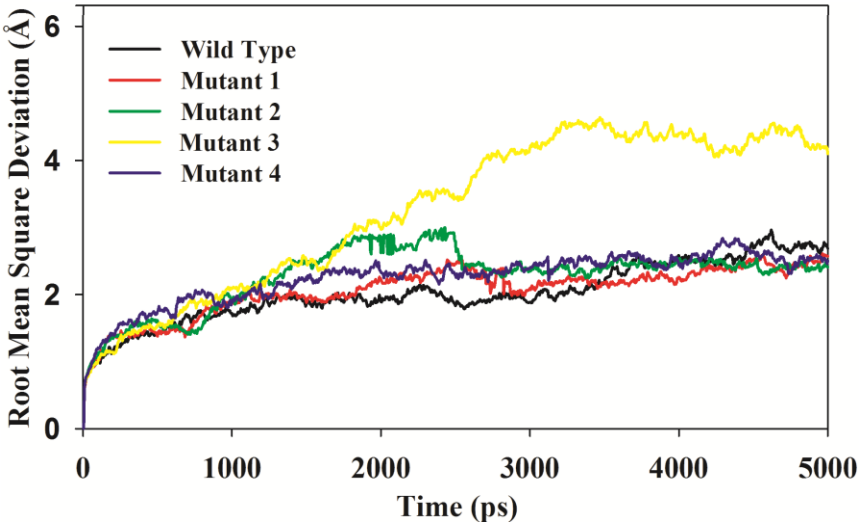

Figure 5: Root mean square deviation (RMSD) of α-β-γ-tubulin complex and the mutants estimated over 5 ns. The RMSD was very stable after the initial 2 ns.

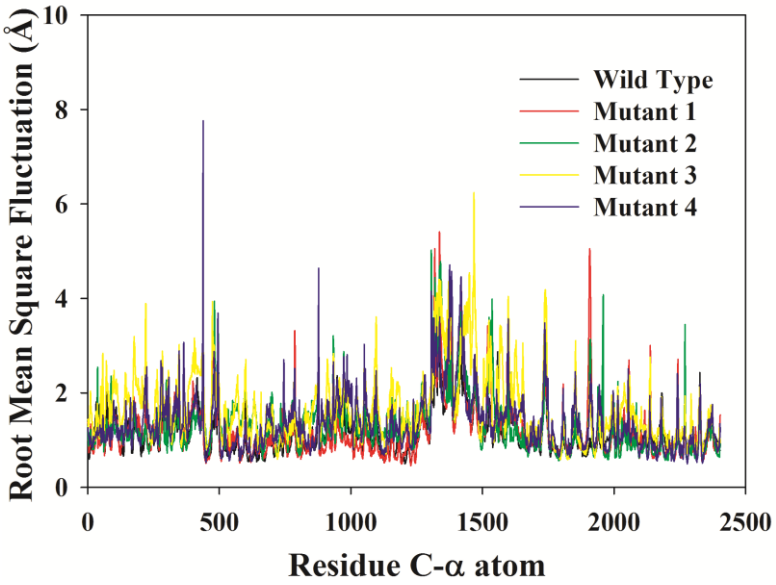

Figure 6: Root mean square fluctuation (RMSF) of α-β-γ-tubulin complex and the mutants estimated over 5 ns.

We also performed root mean square fluctuation (RMSF) of α-β-γ-tubulin complex and the mutants. RMSF of most of the residues was well below 4 Å and only two residues had RMSF >6 (Figure 6). This indicates that the complexes were quite stable throughout the 5 ns simulation.

Calculation of binding free energy between γ-tubulin and microtubules

The calculation of binding free energy between the ligand and the complex of GCP4 and γ-tubulin was carried out on 200 frames, obtained every 10 ps from last 2ns of simulation, using the MM-GBSA and MM-PBSA method. The results are summarized in table 1. The ensemble average of binding free energy using MM-PBSA and MM-GBSA was determined as -110.86 kcal/mol and -120.42kcal/mol. The difference in the values obtained could be attributed to the calculated polar solvation energy which was -1863.37 kcal/mol obtained by MM-GBSA, higher than -1853.81 kcal/mol as obtained using MM-PBSA. All molecular interactions in polar solvent are guided by polar (the polar interaction, $\Delta G_{(ele,PB/GB)} = \Delta E_{ele} + \Delta G_{(PB/GB)}$) and non-polar energy components. The non polar component generally yields a more favourable contribution as compared to the polar component to the molecular interactions as the non-polar residues have the tendency to bury themselves in the hydrophobic pockets allowing the water in the binding site to displace [32]. As observed from table 1, though the desolvation component ($\Delta G_{PB/GB}$) of -1821.50 kcal/mol and -

1824.19 kcal/mol calculated by MM-PBSA and MM-GBSA method respectively, is highly favourable to binding, it cannot compensate the large penalty imposed by the Coulombic contributions ΔE_{ele} of 2027.56 kcal/mol. The non-polar components comprising of van der Waals interaction contribution (ΔE_{vdw}) and the non-polar solvation contribution ($\Delta G_{sol\text{-}np}$) were estimated to be highly favourable with the values of -284.61 kcal/mol and -32.31 kcal/mol, respectively.

Table 1: Calculated binding free energy between α/β tubulin and γ-tubulin. Binding free energy calculated using MM-GBSA and MM-PBSA to ascertain the strength of interaction between α/β tubulin and γ-tubulin. The major energy components like van der Waals, electrostatic, polar solvation and non-polar solvation, contributing to the binding free energy were also estimated.

Contribution	Complex(kcal/mol)
ΔE INT	0.00
ΔEVDW	-284.61
ΔE ELE	2027.56
ΔE GAS	1742.95
ΔG PB	-1821.50
ΔG SOL-NP	-32.31
ΔG SOLV,PB	-1853.81
ΔG ELE,PB	206.06
H TOT,PB	-110.86
G GB	-1824.19
G SOLV,GB	-1863.37
G ELE GB	203.37
H TOT, GB	-120.42

Per-residue energy decomposition

Energy contribution of each residue in the interface between α/β tubulin and γ-tubulin was calculated using the MM-GBSA method to investigate the details of protein-protein interactions at the atomic level (Figure 7). We identified 15 hotspot amino acids that have the highest impact (per residue contribution > 2 kcal/mol) on the α/β tubulin and γ-tubulin interaction interface (Table 2).

Table 2. Decomposition of calculated ΔGbind, GB (kcal/mol) on per residue basis into van der Waals, electrostatic, polar solvation and non-polar solvation energy components. A total of 15 residues with energy contribution of >-2kcal/mol were obtained. The table also includes amino acids with energy contribution > -1 kcal/mol.

Residue	$\Delta E_{i,vdw}$ (kcal/mol)	$\Delta E_{i,ele}$ (kcal/mol)	$\Delta G_{i,sol\ GB}$(kcal/mol)	$\Delta G_{i,sol\text{-}np}$ (kcal/mol)	$\Delta H_{i,tot,GB}$ (kcal/mol)
ARG211	-1.65	214.84	213.64	-0.46	-3.31
ASP215	-1.18	197.66	-197.92	-0.30	-1.74
ARG216	-1.23	250.77	240.94	-0.40	-11.46
HIE218	-5.96	-8.84	10.98	-0.90	-4.72
GLN220	-2.64	-8.92	10.72	-0.82	-1.66
THR276	-3.54	-1.29	2.94	-0.43	-2.32
THR277	-3.17	-1.70	3.92	-0.58	-1.52
ASP278	-1.81	191.34	-191.41	-0.16	-2.05
SER280	-0.52	-2.43	1.87	-0.28	-1.36
GLN298	-1.30	-9.85	9.39	-0.25	-2.01
PRO299	-1.87	-5.26	6.25	-0.24	-1.12
ARG308	-3.58	214.08	216.23	-0.41	-1.83
ARG310	-2.28	269.13	263.88	-0.56	-8.08
GLN311	-4.23	-2.91	5.94	-0.73	-1.93
THR312	-1.59	-0.89	1.25	-0.22	-1.45
ASN313	-0.55	-5.02	4.65	-0.14	-1.07
ARG340	-4.69	198.83	201.26	-0.77	-3.03
PHE347	-3.44	-1.30	0.44	-0.37	-4.68
PRO349	-3.43	-1.92	2.60	-0.48	-3.25
TRP350	-1.31	-1.89	1.67	-0.08	-1.61
PRO352	-2.98	-3.10	3.77	-0.43	-2.73
ALA353	-1.67	-3.49	3.71	-0.28	-1.74
ILE355	-1.17	-0.35	0.46	-0.14	-1.20
ARG389	-0.60	-217.28	212.97	-0.31	-5.22
PRO440	-3.45	-4.69	5.66	-0.58	-3.05
SER444	-1.90	-7.06	7.01	-0.48	-2.44
TRP445	-2.49	161.26	-164.68	-0.60	-6.51

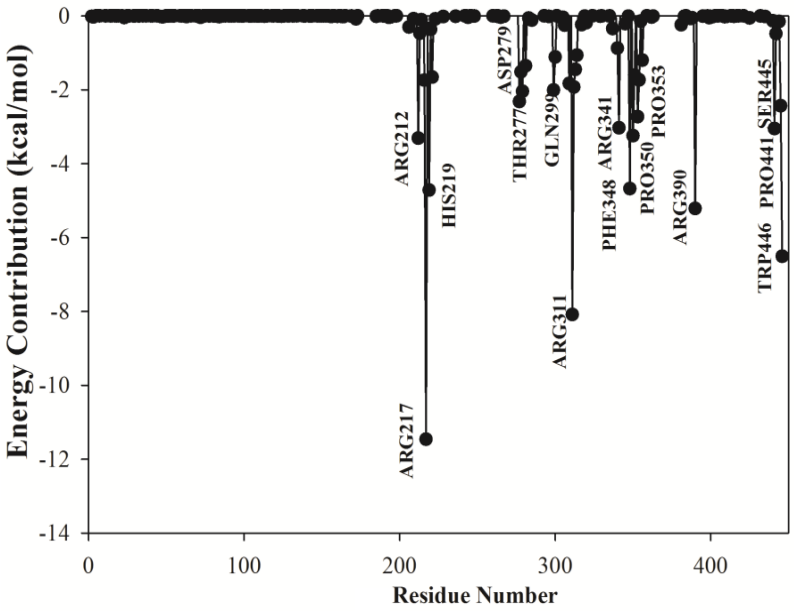

Figure 7: **Per residue free energy contribution of residues in the binding process of GCP4 and γ-tubulin.** Free energy contribution of each residue on the surface between α/β tubulin and γ-tubulin calculated based on MM-GBSA. Only the residues contributing free energy of > -2 kcal/mol (designated as hotspot amino acids) are labelled in the figure.

Table 3: Ensemble average of binding free energy (kcal/mol) of γ-γ tubulin complex calculated using the MM-GBSA and MM-PBSA methods in Amber.

Complex	MM-GBSA (kcal/mol)	MM-PBSA (kcal/mol)
Wild Type	-120.49	-110.86
Mutant 1	-96.51	-65.25
Mutant 2	-90.90	-76.32
Mutant 3	-123.02	-119.95
Mutant 4	-79.24	-82.11

Computational Alanine Scanning Mutagenesis

Each of the prepared mutant was MD simulated in Amber for 5 ns. This was followed by calculation of binding free energy (Table 3). We observed that except for Mutant 3, there was very significant drop in the calculated binding affinities for Mutant 1, Mutant 2 and Mutant and Mutant 4, using both MM-PBSA and MM-GBSA methods.

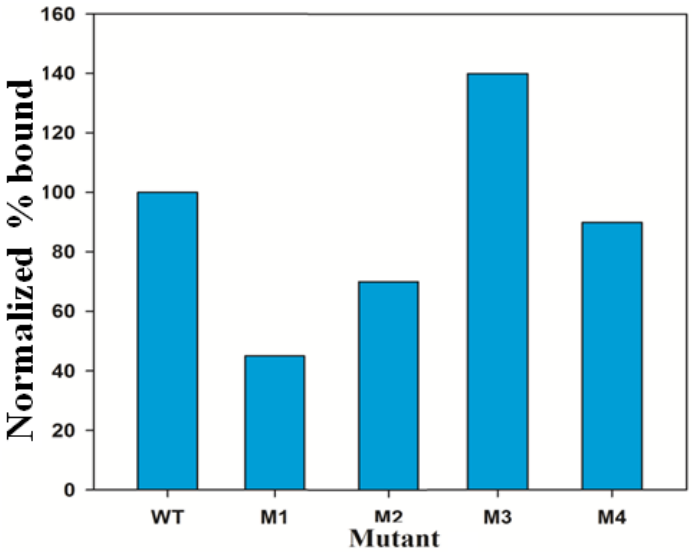

Figure 8: Normalized %bound of α/β tubulin with γ-tubulin.

Growth of Alanine scanning mutant in fission yeast and its phenotype

Since we wished to verify the hot-spot amino acids in order to identify evolutionarily conserved features of γ-tubulin, we took advantage of the fact that the human γ-tubulin gene (*TUBG1*) can replace the fission yeast γ-tubulin (*gtb1*). Using alanine-scanning mutagenesis a series of four mutants of γ-tubulin, as described in figure 6.4, which targeted key residues predicted to be involved in protein-protein interactions, were generated. To test the effect of the alanine substitution on protein function haploid yeast cells, wild-type and *gtb1*-, were transformed with the alanine mutants. Wild-type *TUBG1* transformants served as controls. Radiolabeled γ-tubulin was synthesied in vitro using TnT® Coupled Reticulocyte Lysate System (Promega Corp., Madison WI). The radiolabeled γ-tubulin was then purified using Myc antibody. Finally, *In vitro* microtubule binding assay was performed as described by Li and Joshi (1995) with γ-tubulin and its mutant proteins [33]. The % bound of Wild Type was normalized to 100% (Figure 6.10). The % bound of Mutant 1 (M1), Mutant 2 (M2) and Mutant 4 (M4) was less than the Wild type while that of Mutant 3 (M3) was more than the Wild Type. These experimental results corroborate with the computation alanine scanning data.

Conclusion

The binding interface of γ-tubulin with α/β tubulin was identified using molecular modeling calculations. Residues playing crucial role in the interaction were also identified as hot spot amino acids. To further reinforce the hot spots, computational alanine scanning mutagenesis was

performed. The results were further verified using the experimental alanine scanning mutagenesis. For three of the mutants- M, M2 and M4 the binding affinity was lesser as compared to the wild type as observed after MM-GBSA analysis. Computationally identified interface was well verified by the experimental results.

Acknowledgement:

REFERENCES

[1] C. Wiese and Y. Zheng, "A new function for the γ-tubulin ring complex as a microtubule minus-end cap," *Nature cell biology*, vol. 2, (no. 6), pp. 358-364, 2000.

[2] M. Moritz, M.B. Braunfeld, V. GuÃ©nebaut, J. Heuser, and D.A. Agard, "Structure of the &ggr;-tubulin ring complex: a template for microtubule nucleation," *Nature cell biology*, vol. 2, (no. 6), pp. 365-370, 2000.

[3] T.J. Keating and G.G. Borisy, "Immunostructural evidence for the template mechanism of microtubule nucleation," *Nature cell biology*, vol. 2, (no. 6), pp. 352-357, 2000.

[4] B. Byers, K. Shriver, and L. Goetsch, "The role of spindle pole bodies and modified microtubule ends in the initiation of microtubule assembly in Saccharomyces cerevisiae," *Journal of cell science*, vol. 30, (no. 1), pp. 331-352, 1978.

[5] L.M. Rice, E.A. Montabana, and D.A. Agard, "The lattice as allosteric effector: Structural studies of α/β and γ-tubulin clarify the role of GTP in microtubule assembly," *Proceedings of the National Academy of Sciences*, vol. 105, (no. 14), pp. 5378-5383, 2008.

[6] H. Aldaz, L.M. Rice, T. Stearns, and D.A. Agard, "Insights into microtubule nucleation from the crystal structure of human Î³-tubulin," *Nature*, vol. 435, (no. 7041), pp. 523-527, 2005.

[7] J.M. Kollman, J.K. Polka, A. Zelter, T.N. Davis, and D.A. Agard, "Microtubule nucleating [γ]-TuSC assembles structures with 13-fold microtubule-like symmetry," *Nature*, vol. 466, (no. 7308), pp. 879-882, 2010.

[8] O. Cala, M.-H.l.n. Remy, V.r. Guillet, A. Merdes, L. Mourey, A. Milon, and G. Czaplicki, "Virtual and Biophysical Screening Targeting the γ-Tubulin Complexes "A New Target for the Inhibition of Microtubule Nucleation," *PloS one*, vol. 8, (no. 5), pp. e63908, 2013.

[9] R. Chen, L. Li, and Z. Weng, "ZDOCK: an initialâ€stage proteinâ€docking algorithm," *Proteins: Structure, Function, and Bioinformatics*, vol. 52, (no. 1), pp. 80-87, 2003.

[10] L. Li, R. Chen, and Z. Weng, "RDOCK: Refinement of rigidâ€body protein docking predictions," *Proteins: Structure, Function, and Bioinformatics*, vol. 53, (no. 3), pp. 693-707, 2003.

[11] B. Hess, C. Kutzner, D. Van Der Spoel, and E. Lindahl, "GROMACS 4: Algorithms for highly efficient, load-balanced, and scalable molecular simulation," *Journal of chemical theory and computation*, vol. 4, (no. 3), pp. 435-447, 2008.

[12] W.D. Cornell, P. Cieplak, C.I. Bayly, I.R. Gould, K.M. Merz, D.M. Ferguson, D.C. Spellmeyer, T. Fox, J.W. Caldwell, and P.A. Kollman, "A second generation force field for the simulation of proteins, nucleic acids, and organic molecules," *Journal of the American Chemical Society*, vol. 117, (no. 19), pp. 5179-5197, 1995.

[13] H. Berendsen, J. Postma, W. Van Gunsteren, and J. Hermans, "Intermolecular Forces, ed," *B. Pullman, Reidel, Dordrecht*, vol. 331, 1981.

[14] T. Darden, D. York, and L. Pedersen, "Particle mesh Ewald: An N· log (N) method for Ewald sums in large systems," *The Journal of chemical physics*, vol. 98, (no. 12), pp. 10089-10092, 1993.

[15] U. Essmann, L. Perera, M.L. Berkowitz, T. Darden, H. Lee, and L.G. Pedersen, "A smooth particle mesh Ewald method," *The Journal of Chemical Physics*, vol. 103, (no. 19), pp. 8577-8593, 1995.

[16] J.-P. Ryckaert, G. Ciccotti, and H.J. Berendsen, "Numerical integration of the cartesian equations of motion of a system with constraints: molecular dynamics of< i> n</i>-alkanes," *Journal of Computational Physics*, vol. 23, (no. 3), pp. 327-341, 1977.

[17] D.A. Case, T.E. Cheatham, T. Darden, H. Gohlke, R. Luo, K.M. Merz, A. Onufriev, C. Simmerling, B. Wang, and R.J. Woods, "The Amber biomolecular simulation programs," *Journal of computational chemistry*, vol. 26, (no. 16), pp. 1668-1688, 2005.

[18] D.A. Pearlman, D.A. Case, J.W. Caldwell, W.S. Ross, T.E. Cheatham III, S. DeBolt, D. Ferguson, G. Seibel, and P. Kollman, "AMBER, a package of computer programs for applying molecular mechanics, normal mode analysis, molecular dynamics and

free energy calculations to simulate the structural and energetic properties of molecules," *Computer Physics Communications*, vol. 91, (no. 1), pp. 1-41, 1995.

[19] P.A. Kollman, I. Massova, C. Reyes, B. Kuhn, S. Huo, L. Chong, M. Lee, T. Lee, Y. Duan, and W. Wang, "Calculating structures and free energies of complex molecules: combining molecular mechanics and continuum models," *Accounts of chemical research*, vol. 33, (no. 12), pp. 889-897, 2000.

[20] I. Massova and P.A. Kollman, "Combined molecular mechanical and continuum solvent approach (MM-PBSA/GBSA) to predict ligand binding," *Perspectives in Drug Discovery and Design*, vol. 18, (no. 1), pp. 113-135, 2000.

[21] D. Sitkoff, K.A. Sharp, and B. Honig, "Accurate calculation of hydration free energies using macroscopic solvent models," *The Journal of Physical Chemistry*, vol. 98, (no. 7), pp. 1978-1988, 1994.

[22] T.W. Hendrickson, J. Yao, S. Bhadury, A.H. Corbett, and H.C. Joshi, "Conditional mutations in γ-tubulin reveal its involvement in chromosome segregation and cytokinesis," *Molecular biology of the cell*, vol. 12, (no. 8), pp. 2469-2481, 2001.

[23] K. Maundrell, "nmt1 of fission yeast. A highly transcribed gene completely repressed by thiamine," *Journal of Biological Chemistry*, vol. 265, (no. 19), pp. 10857-10864, 1990.

[24] K. Maundrell, "Thiamine-repressible expression vectors pREP and pRIP for fission yeast," *Gene*, vol. 123, (no. 1), pp. 127-130, 1993.

[25] J. Paluh and D. Clayton, "A functional dominant mutation in Schizosaccharomyces pombe RNase MRP RNA affects nuclear RNA processing and requires the mitochondrial-associated nuclear mutation ptp1-1 for viability," *The EMBO journal*, vol. 15, (no. 17), pp. 4723, 1996.

[26] T. Horio, S. Uzawa, M.K. Jung, B.R. Oakley, K. Tanaka, and M. Yanagida, "The fission yeast gamma-tubulin is essential for mitosis and is localized at microtubule organizing centers," *Journal of cell science*, vol. 99, (no. 4), pp. 693-700, 1991.

[27] T. Horio and B.R. Oakley, "Human gamma-tubulin functions in fission yeast," *The Journal of cell biology*, vol. 126, (no. 6), pp. 1465-1473, 1994.

[28] R.A. Laskowski, M.W. MacArthur, D.S. Moss, and J.M. Thornton, "PROCHECK: a program to check the stereochemical quality of protein structures," *Journal of applied crystallography*, vol. 26, (no. 2), pp. 283-291, 1993.

[29] G. Ramachandran, C.t. Ramakrishnan, and V. Sasisekharan, "Stereochemistry of polypeptide chain configurations," *Journal of molecular biology*, vol. 7, (no. 1), pp. 95-99, 1963.

[30] C. Colovos and T.O. Yeates, "Verification of protein structures: patterns of nonbonded atomic interactions," *Protein Science*, vol. 2, (no. 9), pp. 1511-1519, 1993.

[31] D. Eisenberg, R. Lüthy, and J.U. Bowie, "VERIFY3D: assessment of protein models with three-dimensional profiles," *Methods in enzymology*, vol. 277, pp. 396, 1997.

[32] C.J. Tsai and R. Nussinov, "Hydrophobic folding units at protein-protein interfaces: Implications to protein folding and to protein-protein association," *Protein Science*, vol. 6, (no. 7), pp. 1426-1437, 1997.

[33] Q. Li and H.C. Joshi, "gamma-tubulin is a minus end-specific microtubule binding protein," *The Journal of cell biology*, vol. 131, (no. 1), pp. 207-214, 1995.